BOREAL ENVIRONMENT RESEARCH 9: 447–456 ISSN 1239-6095
Helsinki 22 October 2004

Optical properties of coastal waters of northwestern Estonia: *in situ* measurements

Liis Sipelgas[1)], Helgi Arst[2)], Urmas Raudsepp[1)], Tarmo Kõuts[1)] and Antti Lindfors[3)]

[1)] *Marine Systems Institute TUT, Akadeemia Rd 21, Tallinn 12618, Estonia*
[2)] *Estonian Marine Institute UT, Mäealuse 10a, Tallinn 12618, Estonia*
[3)] *Department of Physical Sciences, P.O. Box 64, Gustaf Hällströmin katu 2, FIN-00014 University of Helsinki, Finland*

Sipelgas, L., Arst, H., Raudsepp, U., Kõuts, T. & Lindfors, A. 2004: Optical properties of coastal waters of northwestern Estonia: *in situ* measurements. *Boreal Env. Res.* 9: 447–456.

A field study of optical properties of the coastal waters of northwestern Estonia was performed from 29 July to 3 August 2002. It was the relaxation period of extensive cyanobacterial bloom in the Gulf of Finland. The concentrations of optically active substances (chlorophyll *a*, coloured dissolved organic matter, suspended matter) and spectrometric light attenuation coefficients were determined from water samples. In addition, continuous measurements of attenuation and absorption coefficients were performed using a flow-through system based on the ac-9 device. The results show that variations of the optical properties of the water masses in the coastal sea of northwestern Estonia are mainly due to changes in the concentration of coloured dissolved organic matter. Water turbidity is well characterized by the slope factor of the scattering coefficient spectrum that is approximated by the power law.

Introduction

The optically active substances (OAS) — suspended matter, coloured dissolved organic matter and phytoplankton pigments — determine the light attenuation properties in the water column. The composition and concentrations of the OAS vary considerably over short distances in seas such as the Baltic Sea, thus resulting in spatial variations of light attenuation characteristics (Højerslev 1988, Siegel *et al*. 1994)

In the present study, the variations of the OAS as well as light attenuation characteristics at the southern part of the entrance to the Gulf of Finland of the Baltic Sea were described based on field measurements. The role of the different OAS in light attenuation characteristics was analyzed.

Field measurements were carried out in coastal waters of northwestern Estonia from 29 July to 2 August 2002 (Fig. 1). The study region included the archipelago (Moonsund) and coastal sea (northwestern coast of Estonia) areas, thus comprising the transition zone between two different types of water masses. Moonsund is influenced by river inflow that discharges nutrients, organic and inorganic suspended material and dissolved organic substances into the sea. The particular location of the coastal sea belongs to the area of strong hydrodynamic and biological variability (Suursaar *et al*. 1995, Pavelson *et al*. 1999).

The measurement programme included: (1) laboratory measurements of the concentrations of chlorophyll *a* and suspended matter from

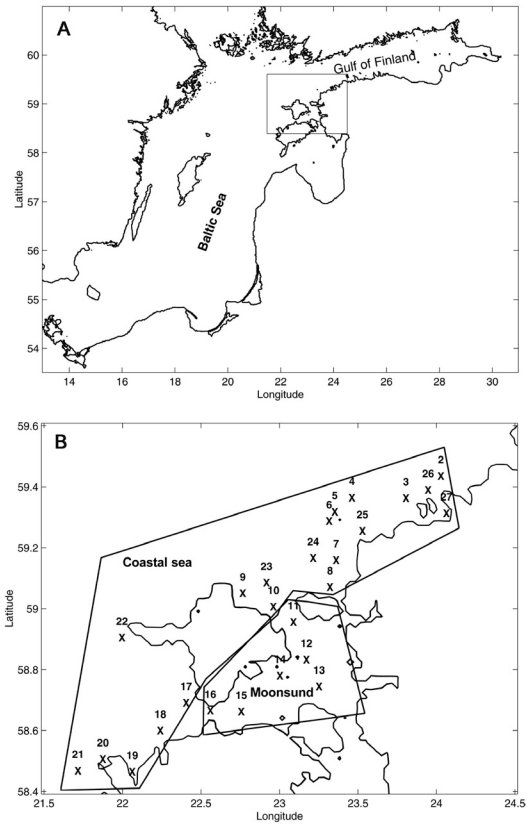

Fig. 1. — **A**: Study site. — **B**: sampling stations.

water samples, (2) laboratory measurements of the light attenuation spectra of filtered and unfiltered water from water samples, and (3) continuous *in situ* measurements of light attenuation and absorption coefficients along the ship route by the flow-through system.

Methods

Laboratory analysis

Concentration of chlorophyll *a* (C_{chl}, mg m^{-3}) was determined by filtering the water samples through Whatman GF/C glass microfibre filters (pore size 1.2 μm, diameter 47 mm, Whatman International Ltd. Maidstone, England), extracting the pigments with hot ethanol (90% at 75 °C) and measuring the absorption at the wavelengths of 665 nm and 750 nm. The values of C_{chl} were calculated with the Lorenzen (1967) formula.

For determination of the suspended matter concentrations the water samples were filtered through pre-weighted Millipore membrane filters (pore size 0.45 μm, diameter 47 mm, Millipore Corporation, Bedford, MA), and the filters were dried to a constant weight at a fixed temperature (103–105 °C). The increase of filter weight indicated the suspended matter concentration in the water sample (Lindell *et al*. 1999).

Spectral measurements in laboratory

The beam attenuation coefficient, c, is a good characteristic of water transparency. However, experimental determination of its true values is complicated. Theoretically, beam transmittance should contain no contribution from scattered light, but in reality small-angle forward scattering does reach the detector. The measured transmittance then exceeds the theoretical value and the attenuation coefficient determined from the measured transmittance is smaller than the true value (Zaneveld *et al*. 1992, Bricaud *et al*. 1995, Arst 2003). Actually, the direct spectrometric reading, $c^*(\lambda)$, for a wavelength λ is the following:

$$c^*(\lambda) = c(\lambda) - Fb(\lambda) - c_d(\lambda), \qquad (1)$$

where $c(\lambda)$ is the beam attenuation coefficient of light for our water sample, $b(\lambda)$ is the light scattering coefficient, $c_d(\lambda)$ is the beam attenuation coefficient of distilled water and F is a coefficient showing the contribution of small-angle forward scattering to the radiation measured by a spectrophotometer (we used Hitachi U1000). We call measured value, $c^*(\lambda)$, "spectrometric attenuation coefficient". Its value is formed under the influence of all three OAS. We measured the spectra of $c^*(\lambda)$ in the range 350–700 nm, recording data with the wavelength increments of 10 nm. The averaged values of c^* over the photosynthetically active region (400–700 nm) were calculated from spectral data. This value integrates the contribution from all OAS to light attenuation.

Water samples were filtered through Millipore membrane filters (pore size 0.45 μm, diameter 47 mm, Millipore Corporation, Bedford, MA) and the corresponding attenuation

spectra were determined for filtered water using a Hitachi U1000. Equation 1 is also valid for filtered water, but the term $Fb(\lambda)$ is practically negligible due to small values of $b(\lambda)$ (including forward scattering). Corresponding values of the spectrometric attenuation coefficient, $c^*_f(\lambda)$, can be used for describing the content of coloured dissolved organic matter (CDOM). The amount of the CDOM is expressed by means of its optical properties. Usually the values of attenuation or absorption coefficients in the violet or blue region of spectrum (380–440 nm) are used (Hickman *et al*. 1984, Althuis *et al*. 1996, Kallio *et al*. 2001, Arst 2003). We measured the spectra of $c^*_f(\lambda)$ in the range 350–700 nm, recording data with the wavelength increments of 10 nm.

The amount of coloured dissolved organic matter can be characterized by its concentration (C_{CDOM}, mg l^{-1}) using the following equation (Højerslev 1980, Mäekivi and Arst 1996, Sipelgas *et al*. 2003):

$$C_{CDOM} = \frac{c^*_f(\lambda)}{\exp(-S(\lambda - \lambda_0))a^*_{CDOM}(\lambda_0)}, \quad (2)$$

where $a^*_{CDOM}(\lambda_0)$ is the specific absorption coefficient of dissolved organic matter, which numerical value at λ_0 = 380 nm at was 0.565 l m^{-1} mg^{-1} (Højerslev 1980), S is the slope parameter equal to 0.017 nm^{-1} (Mäekivi and Arst 1996, Kallio 1999, Sipelgas *et al*. 2003), and $c^*_f(\lambda)$ was taken from spectrometrical reading at λ = 380 nm.

In situ measurements of inherent optical water properties

Inherent optical properties of water were measured using a flow-through system while the vessel was moving. The system was based on the ac-9 instrument (attenuation and absorption meter manufactured by WET Labs Inc.), and it allowed continuous measurements of attenuation (c) and absorption (a) at 9 wavelengths (412, 448, 488, 510, 555, 630, 650, 676, 750 nm). The construction of the system is described in detail in Lindfors and Rasmus (2000). Note that the ac-9 measures the differences $c(\lambda) - c_d(\lambda)$ and $a(\lambda) - a_d(\lambda)$, where $a(\lambda)$ is the absorption coefficient of the water sample at the wavelength λ, and $a_d(\lambda)$ is the absorption coefficient of distilled water at the wavelength λ. The system was calibrated according to the WetLabs user manual. The absorption values were corrected for temperature and light scattering

Results

OAS determined from water samples

Spatial distribution pattern of the OAS concentrations was different for different types of the OAS. Chlorophyll *a* concentration was higher in the coastal sea than in the Moonsund area (Fig. 2a). That can be explained by the fact that the measurements were performed during the relaxation period of rather intensive cyanobacterial bloom. High chlorophyll *a* concentration at certain stations probably indicates filament-like structure of surface accumulations of cyanobacteria. Contrary to this, the content of dissolved organic matter was highest in the Moonsund area, where optical properties of water are strongly influenced by the river inflow (Fig. 2b). No such small-scale irregularities as in the case of chlorophyll *a* concentration were observed. The spatial distribution of suspended matter was also irregular (Fig. 2c) coinciding with chlorophyll *a* distribution in some areas. Relatively high concentration of suspended matter in the western area of our study site was probably due to sediment resuspension in response to a strong wind event on 1 August. Spatial distribution of the spectrometric attenuation coefficient (c^*(400–700)) coincides in general with the CDOM distribution, but indicates some contribution from chlorophyll *a* at the stations with the high chlorophyll *a* content (Fig. 2d). The effect of suspended matter does not emerge in the c^*(400–700) distribution pattern. The values of spectrometric attenuation coefficients at specific wavelength are given in Table 1.

Measurements of light attenuation and absorption spectra

The flow-through system was used during the first two days of the experiment for the measuring of water samples from stations 2–14. At each station, 15–20 series of attenuation and absorp-

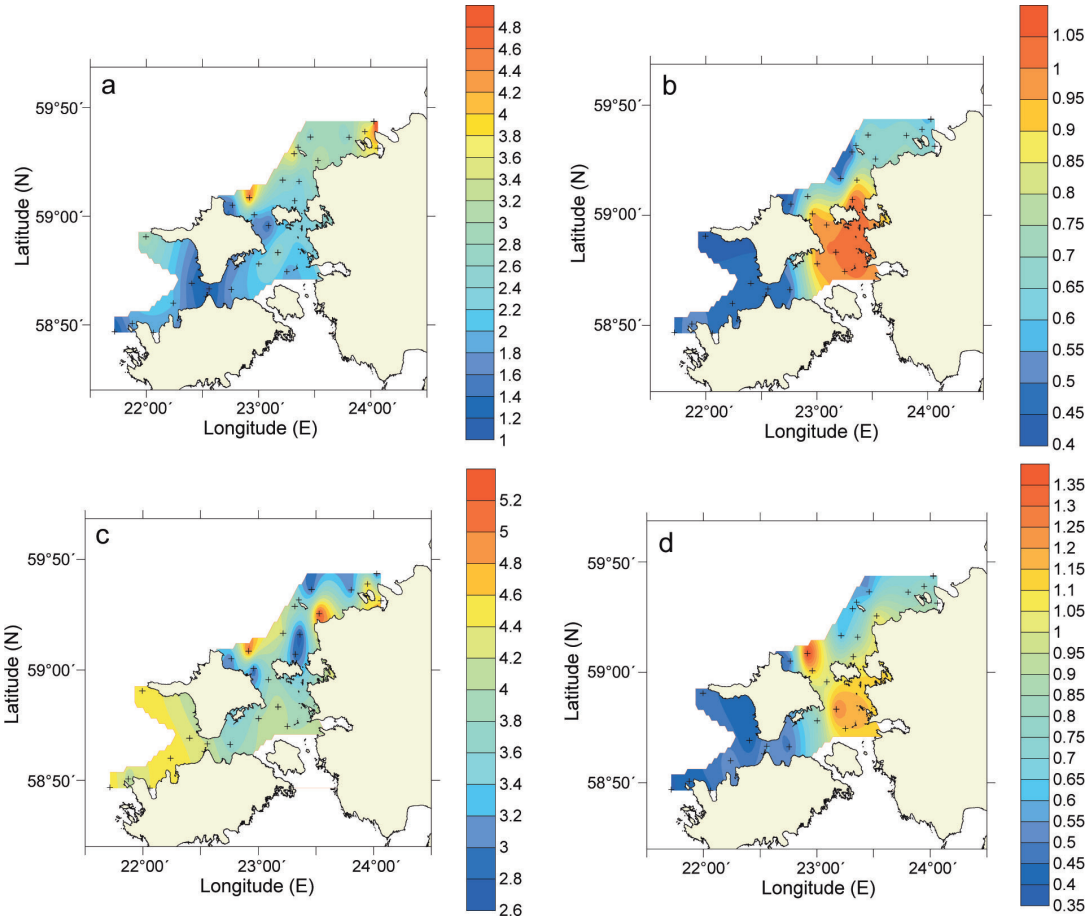

Fig. 2. Spatial distribution of optically active substances along the study site. — **a**: Chlorophyll *a* (mg m^{-3}). — **b**: Coloured dissolved organic matter expressed as spectrometric attenuation coefficient of filtered water at 440 nm (m^{-1}). — **c**: Suspended matter (mg l^{-1}). — **d**: Averaged spectrophotometric attenuation coefficient (m^{-1}).

tion coefficients obtained with the flow-through system were averaged. The values of absorption and attenuation coefficients without the contribution of pure water at water sample stations are presented in Table 2. There is a systematic difference between the attenuation coefficients obtained with the flow-through system and the attenuation coefficients measured in water samples in the laboratory. The attenuation coefficients measured with ac-9 are higher than the spectrometric attenuation coefficients. One of the reasons can be the fact that from Hitachi measurements we get the values c^* (*see* Eq. 1), but from the ac-9 measurements $c - c_d$.

The scattering coefficient was calculated from the attenuation and absorption coefficients:

$$b(\lambda) = c(\lambda) - a(\lambda) \quad (3)$$

The highest attenuation coefficients at 412 nm were observed in the Moonsund area and near the outflow from Moonsund, the stations 8, 10, 11, 12, 13 and 14 (Fig. 3). Absorption coefficient at 412 nm was also more dominant in the same region, showing strong effect of the CDOM, which probably originates from the river water. The distribution of scattering coefficient follows closely the distribution of attenuation coefficient (Fig. 3).

The ratio of absorption coefficient to the scattering coefficient at 412 nm varied from 0.32 to 0.58 indicating that scattering dominates over the absorption in the northwestern Estonian

Table 1. Spectrometric attenuation coefficient $c^*(\lambda)$ (m^{-1}) measured with a laboratory spectrophotometer Hitachi 1000.

Station	700 nm	660 nm	620 nm	580 nm	540 nm	500 nm	460 nm	420 nm	380 nm
2	0.357	0.357	0.364	0.630	0.585	0.704	1.003	1.382	2.309
3	0.405	0.405	0.413	0.586	0.680	0.727	1.051	1.408	2.309
4	0.261	0.309	0.266	0.411	0.467	0.548	0.789	1.098	1.860
5	0.309	0.357	0.364	0.454	0.561	0.727	0.789	1.123	1.920
6	0.405	0.405	0.315	0.454	0.514	0.727	1.003	1.098	1.860
7	0.405	0.405	0.511	0.586	0.633	0.794	1.051	1.564	2.767
8	0.549	0.598	0.610	0.719	0.824	0.975	1.365	1.882	3.141
9	0.213	0.213	0.266	0.367	0.373	0.504	0.695	0.868	1.509
10	0.622	0.671	0.734	0.874	0.969	1.157	1.463	2.150	3.395
11	0.501	0.549	0.561	0.719	0.824	0.975	1.365	1.829	3.173
12	0.720	0.720	0.834	1.009	1.090	1.249	1.660	2.340	3.781
13	0.598	0.622	0.685	0.874	1.017	1.157	1.561	2.150	3.555
14	0.357	0.405	0.413	0.542	0.633	0.794	1.099	1.564	2.798
15	0.213	0.261	0.266	0.411	0.420	0.459	0.647	0.919	1.509
16	0.309	0.309	0.364	0.454	0.514	0.548	0.742	1.046	1.596
17	0.142	0.213	0.218	0.367	0.326	0.459	0.554	0.817	1.509
18	0.261	0.261	0.266	0.411	0.467	0.548	0.742	1.046	1.743
19	0.166	0.166	0.266	0.258	0.420	0.459	0.627	0.970	1.509
20	0.213	0.2013	0.218	0.302	0.373	0.415	0.647	0.868	1.422
21	0.142	0.166	0.193	0.258	0.279	0.371	0.554	0.919	1.422
22	0.213	0.213	0.218	0.302	0.373	0.459	0.647	0.995	1.509
23	0.965	0.965	1.061	1.190	1.385	1.527	1.834	2.259	3.268
24	0.309	0.309	0.315	0.454	0.514	0.615	0.836	1.098	1.860
25	0.549	0.598	0.660	0.830	1.017	1.111	1.365	1.829	2.767
26	0.453	0.453	0.462	0.630	0.680	0.839	1.147	1.408	2.309
27	0.501	0.501	0.561	0.630	0.728	0.839	1.099	1.512	2.369

Table 2. Absorption and attenuation coefficients (m^{-1}) measured with ac-9.

Station	*a*(412)	*a*(440)	*a*(488)	*a*(510)	*a*(555)	*a*(630)	*a*(650)	*a*(676)	*a*(715)
2	1.2746	0.9209	0.4899	0.3487	0.1887	0.0931	0.0891	0.1476	0
3	1.4374	1.0617	0.5708	0.3961	0.2167	0.1216	0.1177	0.1855	0
4	1.1061	0.7909	0.4122	0.2903	0.1541	0.0854	0.0798	0.1183	0
5	1.1779	0.8409	0.4455	0.3151	0.1693	0.0866	0.0814	0.1192	0
6	1.1137	0.8234	0.4655	0.3376	0.1835	0.1058	0.1048	0.1425	0
7	1.42060	0.9364	0.4075	0.2585	0.1257	0.0647	0.0626	0.0930	0
8	1.8410	1.2688	0.6186	0.4354	0.2303	0.1109	0.0920	0.1190	0
9	0.7612	0.4950	0.1805	0.1210	0.0677	0.0474	0.0556	0.0600	0
10	1.8823	1.2840	0.6229	0.4318	0.2164	0.1070	0.1037	0.1891	0
11	1.8323	1.2702	0.6329	0.4472	0.2395	0.1216	0.1214	0.1676	0
12	1.8274	1.2510	0.6022	0.4211	0.2181	0.1045	0.1035	0.1426	0
13	2.0596	1.4336	0.7459	0.5437	0.3223	0.1554	0.1237	0.1352	0
14	1.7526	1.2017	0.6415	0.4705	0.2783	0.1323	0.1019	0.0797	0
	c(412)	*c*(440)	*c*(488)	*c*(510)	*c*(555)	*c*(630)	*c*(650)	*c*(676)	*c*(715)
2	3.7545	3.3035	2.8329	2.6984	2.4881	2.1870	2.1091	2.0454	1.9634
3	4.4756	4.0088	3.4777	3.3158	3.0503	2.7258	2.6463	2.5806	2.4882
4	3.2606	2.8396	2.3845	2.2461	2.0188	1.7416	1.6737	1.6239	1.5365
5	3.4665	3.0331	2.5832	2.4532	2.2504	1.9675	1.8932	1.8411	1.7578
6	4.5907	4.2164	3.8140	3.6865	3.4738	3.2016	3.1232	3.0652	2.9920
7	4.5532	3.9234	3.2258	3.0075	2.6689	2.2995	2.2052	2.1444	2.0256
8	5.7427	4.9945	4.1163	3.8422	3.4175	2.9251	2.8078	2.7149	2.5667
9	3.1132	2.7448	2.3473	2.2048	2.0163	1.7883	1.7391	1.7119	1.6403
10	5.4214	4.7150	3.9591	3.7361	3.4165	3.0577	2.9684	2.9008	2.8080
11	4.9537	4.2143	3.3829	3.1338	2.7619	2.3477	2.2499	2.1793	2.0611
12	5.5585	4.8402	4.0691	3.8465	3.5003	3.1108	3.0078	2.9256	2.8239
13	5.9511	5.2275	4.4773	4.2584	3.9434	3.6058	3.5274	3.4702	3.4047
14	5.0125	4.4054	3.8072	3.6268	3.3976	3.1621	3.0832	3.0184	2.9976

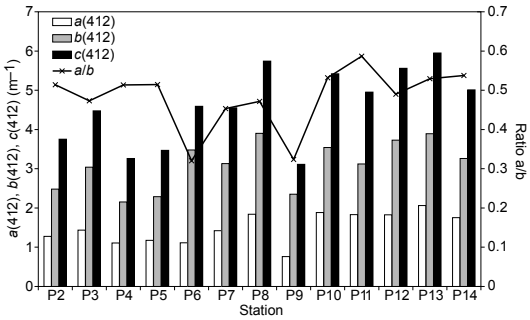

Fig. 3. Values of attenuation coefficient $c(412)$, absorption coefficient $a(412)$ and scattering coefficient $b(412)$ at waveband 412 nm in stations 2–14.

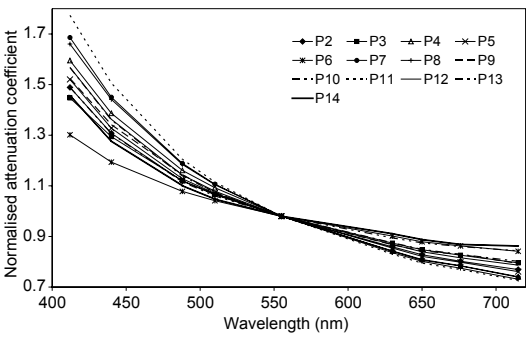

Fig. 4. Spectra of normalised attenuation coefficient in stations 2–14.

coastal sea. The smallest value of this ratio, 0.32, was obtained for station 6 (Fig. 3). There, some surface floating cyanobacteria were visible and that is also seen in representative chlorophyll *a* concentration (Fig. 2a). Note that the opposite result was obtained for the Pohja Bay of the Gulf of Finland (Lindfors and Rasmus 2000), where absorption was a dominant factor in the attenuation at shorter wavelengths.

Change in shapes of attenuation (absorption and scattering) spectra reveals the change in relative concentrations of the OAS (Dekker 1993). The shapes of $c(\lambda)$ spectra varied only slightly in our study area, except for station 6 where the $c(\lambda)$ spectrum had more smooth slope towards shorter wavelength as compared with that for the other stations (Fig. 4). Some difference in the shapes of $c(\lambda)$ spectra was also observed at stations 13 and 14, which had higher $c(\lambda)$ values in the red part of spectrum in comparison with other stations. Those stations were located in the central part of the Moonsund area. Thus, relative concentrations

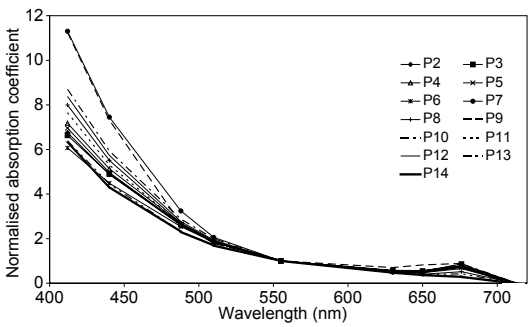

Fig. 5. Spectra of normalised absorption coefficient in stations 2–14.

of the OAS are rather similar in the waters of the northwestern Estonian coastal sea.

The shapes of absorption coefficient spectra also varied slightly from station to station. Only the spectra of stations 7 and 9 were different from the others, giving strong increase towards shorter wavelengths (Fig. 5). Thus, relative concentrations of the OAS differ from those at the other stations. Those stations had the lowest chlorophyll *a* content (Fig. 2a) and the absorption is probably mainly caused by the CDOM, as the influence of the CDOM on the optical properties of water is at its maximum in the violet and blue regions of the spectrum.

Discussion

Relations between IOP and optically active substances

The results in the coastal sea of northwestern Estonia show that the water IOP is related to the CDOM. The spatial distribution of the integrated spectrometric attenuation coefficient $c^*_f(400–700)$ coincides with the CDOM distribution determined as the spectrometric light attenuation coefficient of filtered water at 440 nm. Usually, the amount of the CDOM is characterized by the light absorption coefficient at the low wavelength. Linear regression between the absorption coefficient at 440 nm and the attenuation coefficient of filtered water at 440 nm measured with the laboratory spectrophotometer was

$$a(440) = 1.6473c^*_f(440) + 0.0954 \qquad (4)$$

with correlation coefficient R = 0.89 (Fig. 6). Spectrometric attenuation coefficient can be converted to the CDOM concentration with Eq. 2. Linear regression between the absorption coefficient at 412 and the CDOM concentration was

$$a(412) = 0.4288C_{CDOM} + 0.1603 \quad (5)$$
correlation coefficient $R = 0.94$.

Some authors (Claustre *et al*. 2000, McKee *et al*. 2003) found linear correlation between the absorption at 676 nm and the chlorophyll content in water. However, our data did not confirm this relationship (correlation coefficient between these parameters was only 0.18).

Scattering is known to be a proxy for the suspended matter content in water, Herlevi (2002) found the correlation (R = 0.85) between the average total scattering (over ac-9 wavelengths) and the concentration of suspended matter for Finnish and Estonian lakes. In case of our data, the averaged scattering coefficient did not give such a good correlation, but there was some correlation (R = 0.55) between the suspended matter concentration and the scattering coefficient at wavelength 715 nm. Corresponding linear regression formula is

$$C_{SM} = 0.538b(715) + 2.0683 \quad (6)$$

According to several authors, the shape of the scattering coefficient spectrum, $b(\lambda)$ is influenced by water turbidity (Khalturin 1983, Arst *et al*. 1997, Herlevi *et al*. 1999, Herlevi 2002). The scattering coefficient spectra are well approximated with the power law:

$$b(\lambda) = b_0(\lambda_0/\lambda)^n \quad (7)$$

where b_0 is the scattering coefficient at some reference wavelength λ_0 and n is the slope of the scattering coefficient spectrum, Jerlov and Steemann Nielsen (1974) showed that the wavelength dependence of b becomes weaker with increasing turbidity and the value of n for the Baltic waters is close to zero. According to Herlevi (1999, 2002) in lakes sometimes the opposite conclusion is valid. For instance, in the nordic inland waters he obtained the value of n between 0.13 and 2.42.

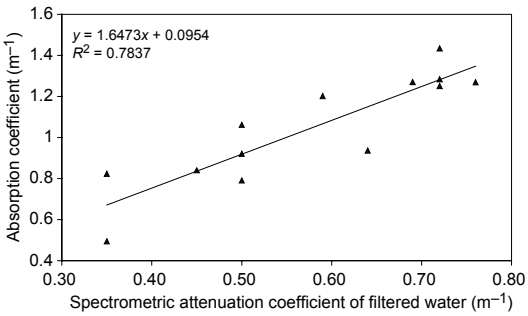

Fig. 6. Correlation between absorption coefficient at 440 nm measured with ac-9 and spectrometric attenuation coefficient of filtered water (440 nm).

The values of n were determined from 20 000 scattering spectra measured with the flow-through system on the route of the ship. The slope factors for scattering curves varied from 0.18 to 0.87 (Fig. 7a). Low values of the slopes were obtained for the Moonsund area and in the northern stations where some surface accumulation of cyanobacteria was visible. As seen on the Modis image, the regions with the lower slopes correspond to the areas of more turbid water (Fig. 7b). The correlation between slope n and concentration of suspended matter at sampling stations was checked and the following regression formula obtained:

$$C_{SM} = 1.475n + 4.1516, \quad (8)$$

where the coefficient of determination was 0.2989 (Fig. 8).

Regression analysis

Combining the data from the flow-through system and from the laboratory analysis of water samples suggests that the relative concentrations of the OAS are rather similar in the coastal waters of northwestern Estonia and the CDOM has major influence on the light attenuation.

We analyzed the data from the water sample stations for evaluating the dependence of spectrometric attenuation coefficient on the different OAS by applying regression analyses. Main statistics of the spectrometric attenuation coefficient and the concentrations of the CDOM, chlorophyll *a* and suspended matter obtained from the laboratory analyses are presented in Table 3.

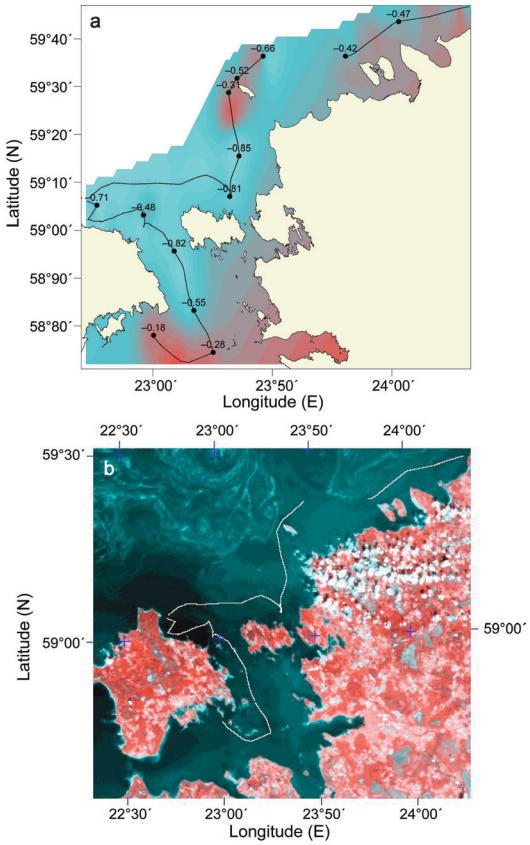

Fig. 7. — **a**: Variation of slope of the scattering coefficient along the ship route. — **b**: RGB (R-band1 (820–860 nm); G-band2 (620–670 nm); B-band2 (620–670 nm)) MODIS (Moderate Resolution Imaging Spectrometer) image, 30 July 2002. Light areas represent the water with higher turbidity.

Simple linear regression analysis indicates that $c^*(400–700)$ does not give good correlation neither with concentrations of suspended matter nor chlorophyll *a* (respective correlation coefficients were 0.078 and 0.35). However, the correlation between $c^*(400–700)$ and the dissolved organic matter was quite evident (R = 0.75).

Table 3. Minimum, maximum and standard deviation of optically active substances.

Parameter	Mininum	Maximum	Mean	S.D.
$c^*(400–700)$ (m^{-1})	0.39	0.80	0.74	0.29
C_{CDOM} (mg l^{-1})	1.76	4.14	2.61	0.80
C_{chl} (mg m^3)	1.14	5.16	2.55	1.06
C_{SM} (mg l^{-1})	2.10	5.40	3.93	0.79

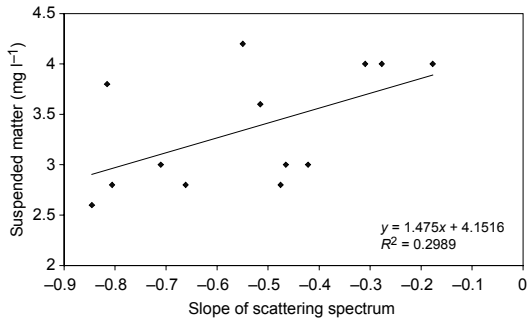

Fig. 8. Correlation between suspended matter concentration and slope of scattering spectrum.

Common knowledge is that variations of optical properties of the water masses of the Baltic Sea are mainly determined by the concentration of the CDOM. Still, all three types of optically active substances simultaneously affect the light attenuation. Thus, the multiple regression analysis was applied to study our data.

We used standardized variables to exclude the dependence the coefficients of the formula on measurement units. The standardized value for each variable is obtained as

$$x_s = \frac{x - \bar{x}}{\sigma_x}, \qquad (9)$$

where x_s is the standardized value of variable x, $\bar{x}$ is sample mean and σ_x is standard deviation of x. The values from Table 3 were used for means and standard deviations. As a result we obtained the following multiple regression formula:

$$c^*_s(400–700) = 0.3C_{SM.s} + 0.35C_{chl.s} + 0.86C_{CDOM.s}. \qquad (10)$$

The multiple correlation coefficient was 0.9 and all coefficients in (Eq. 8) are different from zero at 95% confidence level.

From Eq. 10 we can see that changes in $c^*(400–700)$ are mostly caused by changes in the CDOM, while the effect of changes in suspended matter and chlorophyll *a* are close to each other. For instance, the increase of $c^*(400–700)$ by 1 m^{-1}, could be explained by the increase of the CDOM of 3.3 mg l^{-1}, or C_{chl} *a* of 10 μg l^{-1} or suspended matter of 9 mg l^{-1}.

Contribution of the different OAS in formation of a numerical value of $c^*(400–700)$ was calculated based on spectral measurements in the

laboratory. From spectral measurements of $c^*_f(\lambda)$ we can find the ratio $c^*_f(400–700)/c^*(400–700)$, which shows the contribution of the CDOM in formation of numerical values of $c^*(400–700)$. Based on the data for 27 stations we found that this ratio varies between 14% and 46%, with the average value of 30%. It leaves the contribution of 54%–86% from chlorophyll *a* and the suspended matter together. Consequently, we can say that all OAS have significant contribution to the light attenuation, while variations of the CDOM have major effect on its changes.

Conclusions

Spatial distribution pattern of the OAS concentrations was different for different types of the OAS in the northwestern Estonian coastal sea. The concentration of the coloured dissolved organic matter was higher in Moonsund due to river inflow as compared with that of the open coastal sea area. Small-scale patches of high concentrations of chlorophyll and suspended matter were mainly in the open coastal sea area due to the remnants of cyanobacteria bloom. The spatial distribution of the spectrometric attenuation coefficient, $c^*(400–700)$, matched the CDOM distribution in general. Multiple regression analysis confirmed that changes in the CDOM concentration have a major effect on the changes of the spectrometric attenuation coefficient.

The analysis of optical properties of seawater showed that the light attenuation and absorption spectra were rather similar in different locations of the northwestern Estonian coastal sea. Also, light scattering dominated over the absorption in the light attenuation. There was strong correlation between the CDOM content in water and absorption at 440 nm, but our data did not show correlation between absorption at 676 and chlorophyll content in water. Suspended matter concentration correlated best with scattering coefficient at 715 nm.

Present analyses confirmed that wavelength dependence of scattering coefficient becomes weaker with increasing water turbidity.

Acknowledgements: This work was partially supported by the Estonian Science Foundation (Grant 5594 and Grant 5596). The authors thank the Estonian Maritime Administration for providing the survey vessel. The authors are also grateful to Gennadi Lessin for preparing figures in the article.

References

Althuis I.J.A., Vogelzang J., Wenard M.R., Shimvell S.J., Gieskes W.W.C., Warnock R.E., Kromkamp J., Wouts R. & Zevenbloom W. 1996. *On the colour of case II waters. Particulate matter North Sea. Part 1: Results and conclusions*. Report NRSP-2, 95-21A: 1–193.

Arst H. 2003. *Optical properties and remote sensing of multicomponental water bodies*. Springer, Praxis Publishing, Chichester, UK: 1–231.

Arst H., Mäekivi S., Lukk T. & Herlevi A. 1997. Calculating irradiance penetration into water bodies from the measured beam attenuation coefficient. *Limnol. Oceanogr.* 42: 379–385.

Bricaud A., Roesler C. & Zaneveld. J.R.V. 1995. In situ methods for measuring the inherent optical properties of ocean waters. *Limnol. Oceanogr.* 40: 393–410.

Claustre H., Fell F., Oubelkheir K. & Prieur L. 2000. Continuous monitoring of surface optical properties across a geostrophic front: Biogeochemical inferences. *Limnol. Oceanogr.* 45(2): 309–321

Dekker A.G. 1993. *Detection of optical water quality parameters for eutrophic waters by high resolution remote sensing*. Ph.D. thesis, Free University, Amsterdam.

Herlevi A. 2002. *Inherent and apparent optical properties in relation to water quality in Nordic waters*. Academic dissertation in geophysics, University of Helsinki, Finland.

Herlevi A., Virta A., Arst H. & Erm A. 1999. Results of light absorption/attenuation measurements in Finnish and Estonian lakes in summer 1997. *Proc. Estonian Acad. Sci. Biol. Ecol.* 48(1): 46–62.

Hickman N.J., McShane P.E. & Axelrad D.M. 1984. Light climate in the Gippsland lakes, Victoria. *Aust. J. Mar. Freshw. Res.* 35: 517–524.

Højerslev N.K. 1980. On the origin of yellow substance in the marine environment. *Oceanogr. Rep., Univ. Copenhagen. Inst. Phys.* 42: 1–35.

Højerslev N.K. 1988. *Natural occurrences and optical effects of Gelbstoff*. University press, Kopenhagen.

Jerlov N.G. & Steemann N.E. 1974. *Optical aspects of oceanography*. Academic Press Inc., New York, London.

Kallio K. 1999. Absorption properties of dissolved organic matter in Finnish lakes. *Proc. Estonian Acad. Sci. Biol. Ecol.* 48: 75–83.

Kallio K., Kutser T., Hannonen T., Koponen S., Pulliainen J., Vepsälainen J. & Pyhälahti T. 2001. Retrieval of water quality from airborne imaging spectrometry of various lake types in different seasons. *Sci. Total. Environ.* 268: 59–77.

Khalturin V.I. [Халтурин В.Й.] 1983. *On the transfer of the light fluxes in vertically homogeneous ocean*. Acad. Sci. Ukrainian SSR, Marine Hydrophysical Institute, Sevastopol, pp. 1–39. [In Russian].

Lindell T., Pierson D., Premazzi G. & Zilioli E. (eds.) 1999. *Manual for monitoring European lakes using remote*

sensing techniques. Luxembourg. European Communities.

Lindfors A. & Rasmus K. 2000. Flow through system for distinguished dynamic features in the Baltic Sea. *Geophysica*. 36: 203–214.

Lorenzen C.J. 1967. Determination of chlorophyll and phaetopigments; spectrophotometric equations. *Limnol. Oceanogr*. 12: 343–346.

McKee D., Cannigham A., Slater J., Jones K.J. & Griffits C.R. 2003. Inherent and apparent optical properties in coastal waters: a study of the Clyde sea in early summer. *Estaurine, Coastal and Self Science*. 56: 369–376.

Mäekivi S. & Arst H. 1996. Estimation of the concentration of yellow substance in natural waters by beam attenuation coefficient spectra. *Proc. Estonian Acad. Sci. Ecol*. 6(3/4): 108–123.

Pavelson J., Kononen K. & Laanemets J. 1999. Chlorophyll distribution patchiness caused by hydrodynamical processes: a case study in the Baltic Sea. *Journal of Marine Science*. 56: 87–99.

Siegel H., Gerth M. & Beckert M. 1994. The variation of optical properties in the Baltic Sea and algorithms for the application of remote sensing data. *SPIE 2258, Proc. Ocean Optics XII*: 894–905.

Sipelgas L., Arst H., Kallio K., Erm A., Oja P. & Soomere T. Optical properties of dissolved organic matter in Finnish and Estonian lakes. *Nordic Hydrology.* 34: 361–386.

Suursaar Ü., Astok V., Kullas T., Nõmm A. & Otsmann M. 1995. Currents in the Suur Straight and their role in the nutrient exchange between the Gulf of Riga and the Baltic Proper. *Proc. Estonian Acad. Sci. Ecol*. 5: 103–123.

Zaneveld J.R.V., Kitchen J.C., Bricaud A. & Moore C. 1992. Analysis of *in situ* spectral absorption meter data. *SPIE 1750, Proc. Ocean Optics XI*: 187–200.

Received 23 November 2003, accepted 2 September 2004